
Graph Neural Network with Automorphic Equivalence Filters

Fengli Xu¹, Quanming Yao^{1,2}, Pan Hui³, Yong Li¹

1) Department of Electronic Engineering, Tsinghua University; 2) 4Paradigm Inc.

3) Department of Computer Science and Engineering, HKUST.

fenglixu2020@hotmail.com, quanmingyao@gmail.com

panhui@cse.ust.hk, liyong07@tsinghua.edu.cn

Abstract

Graph neural network (GNN) has recently been established as an effective representation learning framework on graph data. However, the popular message passing models rely on local permutation invariant aggregate functions, which gives rise to the concerns about their representational power. Here, we introduce the concept of automorphic equivalence to theoretically analyze GNN’s expressiveness in differentiating node’s structural role. We show that the existing message passing GNNs have limitations in learning expressive representations. Moreover, we design a novel GNN class that leverages learnable automorphic equivalence filters to explicitly differentiate the structural roles of each node’s neighbors, and uses a squeeze-and-excitation module to fuse various structural information. We theoretically prove that the proposed model is expressive in terms of generating distinct representations for nodes with different structural feature. Besides, we empirically validate our model on eight real-world graph data, including social network, e-commerce co-purchase network and citation network, and show that it consistently outperforms strong baselines.

1 Introduction

The past few years have witnessed the phenomenal success of GNNs in numerous graph learning tasks [1, 2, 3], which leads to a surge of interests from both academia and industry [4]. Despite of their various architectures, the majority of GNNs apply permutation invariant aggregate function on each node’s local neighborhood to learn node embeddings, which is also known as message passing neural networks (MPNNs) [5]. As a result, the MPNNs cannot differentiate each node’s neighbors, which leads to concerns about their representational power [6, 7]. In this paper, we look at MPNN’s expressiveness from an important and largely overlooked angle, i.e., the capacity to distinguish the structural roles of each node’s neighbors.

Inspired by the *structural role* assumption in social and biology graph analysis [8, 9, 10], we use the concept of automorphic equivalence [11] to differentiate the roles of each node’s neighbor. Specifically, two nodes are considered automorphic equivalence only if they are interchangeable in some index permutations that preserve the connection matrix, i.e., graph automorphisms [12]. It allows us to identify the neighboring nodes that form similar structural patterns as automorphic equivalences, which tend to have similar influence on the ego node according to the *structural role* assumption [9]. However, through theoretical analysis, we prove that current MPNNs, e.g., GCN [1], GraphSAGE [3], GAT [13] and GIN [7], have fundamental limitations in modelling automorphic equivalence nodes, which hinder their capacity in capturing this important structural information.

We further propose GRaph AutomorPhic Equivalent network (GRAPE), a novel GNN class that can extract expressive structural features by differentiating the structural roles of each node’s neighbors.

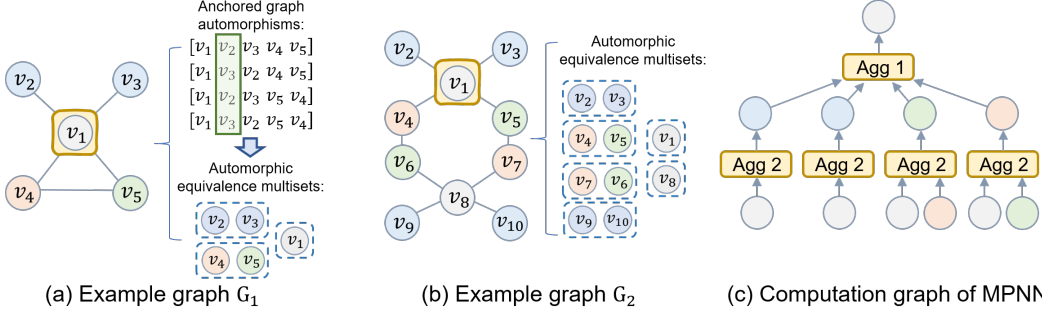


Figure 1: An illustration of the AE multisets in example graphs and the limitations of current MPNNs, where the nodes with same colors have identical features.

Specifically, GRAPE first partitions each node’s neighbors into several automorphic equivalence multisets to model their structural roles. Then, we design a learnable filer to aggregate the node features in these multisets, which adaptively assigns different weights to neighboring nodes with different structural roles and explicitly model the interdependency among them. Moreover, in order to capture complex structural features, GRAPE proposes to first match the neighborhood with pre-defined subgraph templates to form several feature channels, and then fuse the features learned from different channels with a squeeze-and-excitation module [14].

We theoretically prove that the proposed GRAPE framework is expressive in terms of learning distinct representations for nodes with different automorphic equivalence multisets, which fundamentally makes up the shortcomings of current MPNNs. Moreover, we empirically validate GRAPE on eight real-world datasets, which cover the scenarios of social network, citation network and e-commerce co-purchase network. Experiments show GRAPE consistently outperforms all state-of-the-art baseline models with up to 60% accuracy improvement. Besides, case studies indicate GRAPE can effectively differentiate the structural roles of each node’s neighbors.

2 Related Works

2.1 Message Passing Neural Networks (MPNNs)

We represent a graph as $G = (\mathcal{V}, \mathcal{E})$, where $\mathcal{V} = \{v_1, v_2, \dots, v_n\}$ is the set of nodes and $\mathcal{E} = \{(v_i, v_j)\}$ is the set of edges. Let the feature vector of node v_i be $\mathcal{X}(v_i)$, and $\mathcal{N}(v_i)$ represents the set of v_i ’s neighbors in G . Generally, a K -layer message passing neural networks (MPNN) [15, 3, 7] computes the representation for a given node v_t by

$$h^k(v_t) = \text{COMB} (h^{k-1}(v_t), \text{AGG} (\{h^{k-1}(v_j) | v_j \in \mathcal{N}(v_t)\})), \quad \forall k = 1, \dots, K, \quad (1)$$

and $h^0(v_i) = \mathcal{X}(v_i)$, where **AGG** is the *aggregate* function that collects feature from neighboring nodes, and **COMB** is the *combine* function that integrates each node’s self feature with the neighborhood feature. Besides, for graph classification task, there might be a **READOUT** function that computes the graph embedding by integrating all node’s embedding.

Existing MPNNs mainly use local permutation invariant aggregate functions to compute node embeddings, which subsumes a large class of popular GNN models such as GCN [1], GraphSAGE [3], GAT [13], Geniepath [16] and GIN [7]. More recently, several attempts have been made to augment MPNN framework with additional graph structural information [6]. From node’s perspective, *P-GNN* proposed to encode the graph position by measuring each node’s distance to selected anchors [17], while *graph stethoscope* suggest a combination of heterogeneous aggregate functions can better capture graph moments [18]. From edge’s perspective, *CPNGNN* proposed to order the edge of each node with port numbers to better solve combination optimization problems [19], while *DimeNet* [20] was designed to encode the spatial orientation of edges into the passed messages for molecule modelling.

2.2 Automorphic Equivalence (AE) in Graph Analysis

Measuring the structural similarity in graph has been a central topic in the domains of computational biologist, social network analysis and chemoinformatics for a long time [9, 10]. Researchers found

evidences that individual with similar structural patterns in social network tend to have similar social status [21], while proteins tend to exert similar functions if they have high structural similarity in protein-protein interaction network [22]. As a result, several approaches were proposed to map nodes to their functions based on structural similarities, which usually partitioned nodes into structural equivalence sets based on the intuition of “functorial reduction” [9, 23]. Specifically, we use the concept of automorphic equivalence in our study [11], which depends on the definition of graph automorphism as follows [12].

Definition 2.1 *Given a graph $G = (\mathcal{V}, \mathcal{E})$, an **automorphism** $\pi(\star)$ is a permutation of the nodes that preserves the connectivity, i.e., the permuted nodes $\pi(v_a)$ and $\pi(v_b)$ are connected if and only if nodes v_a and v_b are connected.*

In the context of GNN, the ego node v_t itself plays a unique role in learning its embedding [1]. Therefore, we distinguish it from its neighborhood by adapting the concept of automorphic equivalence to the ego-centered setting as follows [11].

Definition 2.2 *Two nodes v_a and v_b are considered to be **ego-centered automorphic equivalence** if there is an anchored graph automorphism $\pi_A(\star)$ that maps one onto the other, i.e., $\pi_A(v_a) = v_b$, where $\pi_A(\star)$ is a graph automorphism with the first node fixed.*

Without explicit mention, the term of *automorphic equivalence* (AE) throughout this paper follows the ego-centered setting.

3 Limitations of Current MPNNs

Recently, an important and popular method to understand the expressiveness of MPNN is through the lens of graph isomorphism test [6, 24]. It has been proven that MPNNs are at most as powerful as Weisfeiler-Lehman test in discriminating graph isomorphism [7]. However, their capacity in capturing the structural roles among different neighbors is still not clear.

We illustrate this problem with an example graph in Figure 1 (a), current MPNNs might reach the conclusion that *blue* nodes are the most important feature in v_1 ’s neighborhood, where the colors of nodes indicate their features. However, v_4 and v_5 might have greater influence on v_1 because they form a triangle structure, which is known to capture the strong ties in social network [25, 26]. On the other hand, such structural information can be captured by AE. We can observe that there are four anchored graph automorphisms, which show certain nodes can be mapped onto each others such as v_3 and v_2 in the green box area. As a result, the nodes can be partitioned into three AE multisets, i.e. $\{v_1\}$, $\{v_2, v_3\}$ and $\{v_4, v_5\}$, which effectively captures the triangle structure formed by v_4 and v_5 .

Therefore, one fundamental question to ask is how does the AE related to graph isomorphism test. In light of MPNN’s local property, we investigate this problem on each node’s k -hop neighborhood. Specifically, two nodes are considered *neighborhood isomorphic* if their k -hop neighborhood are graph isomorphisms [27]. For any k within the graph diameter, there is the following theorem [27].

Theorem 3.1 *Two automorphic equivalence nodes are neighborhood isomorphic, while the converse statement is false.*

A constructive proof of Theorem 3.1 was given in [27]. The main reason is the neighborhood isomorphism does not need to map one ego onto the other, which is a key factor in modelling the neighbor’s influence. Therefore, AE is a strictly stronger condition than graph isomorphism. Moreover, to better understand MPNN’s expressiveness in capturing structural role, we formalize the analytic framework as whether it can discriminate two nodes with different AE multisets in their neighborhood, which leads to the following proposition about the limitations of MPNNs.

Proposition 3.2 *There exist graphs that have different AE multisets for the ego node, but MPNNs described in Equation (1) with arbitrary number of layers and hidden units cannot distinguish them.*

A construction proof of Proposition 3.2 is demonstrated in Figure 1. We can observe that example graphs G_1 and G_2 have different AE multisets for the corresponding ego nodes, but their computation graphs of 2-layer MPNN are exactly the same, which are shown in Figure 1 (c). In fact, since each node in graph G_2 can be mapped to a node in graph G_1 with identical 1-hop neighborhood, MPNNs

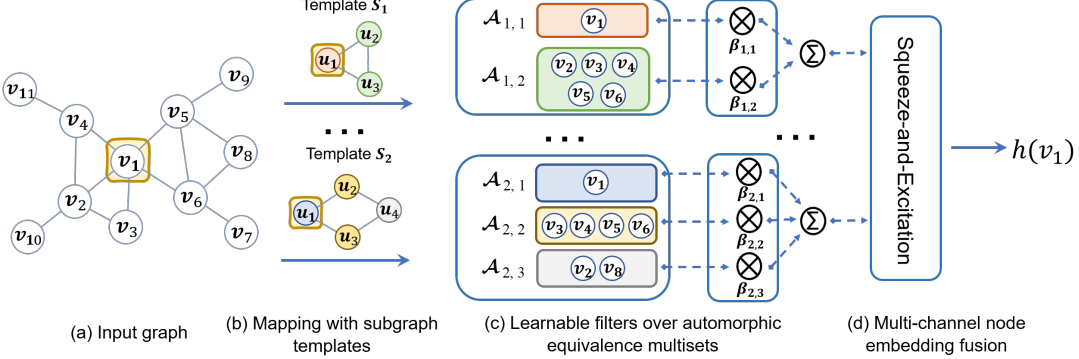


Figure 2: The GRAPE architecture. (a) The input graph with node v_1 as ego node. (b) Mapping node v_1 's neighborhood with given subgraph templates, where nodes with same color are AE. (c) Aggregating features from AE multisets with learnable filters. (d) Fusing multi-channel node embedding with squeeze-and-excitation module.

with arbitrary layers cannot discriminate these two nodes. Therefore, MPNNs have fundamental limitations in modelling the structural role of each node's neighbors.

Finally, in Section 2.1, we show there are some recent works try to distinguish neighbors of a node in MPNN. However, these recent attempts are dedicated to different specific problems, e.g., graph position [17], graph moment [18], spatial orientation of edges in molecules [20]. Although AE is a key property for graph data, it has not been addressed by previous studies. We provide more discussions about their limitations in modelling AE in Appendix A.

4 The Proposed GRAPE Architecture

In this section, we propose GRaph AutomorPhic Equivalence network (GRAPE), a novel framework that explicitly models the structural roles of each node's neighbors via AE multisets. GRAPE is motivated by two key insights. First, the neighbor's structural role can be captured by its membership in the AE multisets. Second, the neighbor's structural role depends on the subgraph pattern it forms with the targeted node. Therefore, we should leverage various subgraph templates to capture all the important structural information. Subsequently, GRAPE contains the following key components:

- 1) A set of subgraph templates $\{S_1, S_2, \dots, S_L\}$, and each subgraph template forms a unique feature channel by deriving different AE multisets from each node's neighborhood.
- 2) AE filters that couple the aggregate functions with the underlying AE multisets, which allows GRAPE to explicitly model structural roles of each node's neighbors.
- 3) A squeeze-and-excitation module to fuse the node embeddings generated via multiple channels.

These components are illustrated in Figure 2, and the overall framework is described in Algorithm 1. In the sequel, we describe them in details.

4.1 Subgraph Templates Matching

The GRAPE framework leverages subgraph templates with different size and connectivity patterns to capture different structural information. Specifically, a subgraph template is denoted as connected graph $S = (\mathcal{U}, \mathcal{R})$, where $\mathcal{U} = \{u_1, u_2, \dots, u_d\}$ is the set of nodes and $r = (u_i, u_j) \in \mathcal{R}$ is the set of edges. Besides, u_1 is a unique node that always maps to the ego node v_t . Given a subgraph template, we first need to identify the AE nodes on it, which can be efficiently computed with the well-known *nauty* algorithm [12]. For example, as illustrated in Figure 2(b), the template S_1 has two anchored graph automorphisms $[u_1, u_2, u_3]$ and $[u_1, u_3, u_2]$. Therefore, there are two sets of AE nodes in template S_1 , i.e., $\{u_1\}$ and $\{u_2, u_3\}$. Then, we can partition each node's neighbors into AE multisets by mapping them onto the subgraph template. Specifically, the subset of nodes in graph G is considered a match instance to subgraph template S if it preserves all the connections in it, which captures the *functional motif* in graph analysis [28]. To efficiently match each node's neighborhood, we design a backtracking matching algorithm that is detailedly described in the Appendix B.

Algorithm 1: GRaph AutormorPhic Equivalent Network (GRAPE)

Input: Input graph $G = (\mathcal{V}, \mathcal{E})$, node feature $\mathcal{X}(v)$, AE multisets $\{\mathcal{T}_1, \dots, \mathcal{T}_L\}$ for L subgraph templates, layer $k \in [1, K]$, learnable functions $\psi(\cdot)$, $\text{AGG}(\cdot)$, non-linearity $\sigma(\cdot)$;

Output: Node embedding $h(v)$;

- 1 $h^0(v) \leftarrow \mathcal{X}(v), \forall v \in \mathcal{V}$
- 2 **for** $k \in 1, \dots, K$ **do**
- 3 # Automorphic equivalence filter with various subgraph templates
- 4 **for** $\mathcal{T}_l \in \{\mathcal{T}_1, \dots, \mathcal{T}_L\}$ **do**
- 5 | Compute $h_l^k(v)$ using Equation (2)
- 6 **end**
- 7 $\mathbf{H}^k = \text{CONCAT}\{h_l^k(v) \mid \forall v \in \mathcal{V}, l \in 1, \dots, L\}$
- 8 # Squeeze-and-excitation module to fuse multi-channel embeddings
- 9 $\gamma^k = \text{GLOBAL_AVERAGE}(\mathbf{H}^k)$
- 10 $\alpha^k = \sigma(\mathbf{W}_2^k \cdot \sigma(\mathbf{W}_1^k \cdot \gamma^k))$
- 11 $h^k(v) = \sum_{l=1, \dots, L} \alpha^k[l] \cdot h_l^k(v), \text{ for } v \in \mathcal{V}$
- 12 **end**
- 13 Return $h^K(v)$

4.2 Automorphic Equivalence (AE) Filter

Inspired by the learnable filters in CNN [29], we design a learnable AE filter to model the AE multisets in each node’s neighborhood. Specifically, given a node v_t and subgraph template S_l , we denote its AE multisets as $\mathcal{T}_l = \{\mathcal{A}_{l,1}(v_t), \dots, \mathcal{A}_{l,j}(v_t), \dots, \mathcal{A}_{l,m_l}(v_t)\}$, where $\mathcal{A}_{l,j}(v_t)$ is the multiset of nodes corresponding to the j -th sets of AE nodes in S_l and m_l is the total number AE multisets. Then, v_t ’s node embedding $h_l^k(v_t)$ can be computed as follows:

$$h_l^k(v_t) = \psi \left(\sum_j \beta_{l,j} \cdot \text{AGG}(\{h_l^{k-1}(v_n) \mid v_n \in \mathcal{A}_{l,j}(v_t)\}) \right), \quad (2)$$

where $\text{AGG}(\cdot)$ is a learnable function that aggregates feature from each AE multiset and $\beta_{l,j}$ is a learnable weight that models the importance of the j -th equivalence multiset. Besides, $\psi(\cdot)$ transforms the weighted sum feature into node embeddings. The computation process is illustrated in Figure 2(c). Differs from the local permutation invariant MPNNs, the proposed AE filter can explicitly differentiate the neighboring nodes with different structural roles by assigning different weights $\beta_{l,j}$ to them. It allows GRAPE to filter out the combination of important AE multisets and effectively models the interdependency among them, which resembles the learnable filter in CNN. Note that GRAPE does not have an explicit *COMBINE* function to account for the ego node’s self feature. However, the ego node v_t will always be captured in a unique AE multiset, such as the $\mathcal{A}_{1,1}$ and $\mathcal{A}_{2,1}$ in Figure 2(c), which allows GRAPE to implicitly integrate the ego node’s self feature.

4.3 Fusing Multi-channel Embeddings

By leveraging a set of various subgraph templates $\{S_1, S_2, \dots, S_L\}$, GRAPE can learn multiple AE filters accordingly to capture different structural information, which forms multiple feature channels. Therefore, it is an important problem to effectively fuse the multi-channel features. One simple solution is to apply averaging pooling among different channels. However, inspired by the channel-wise enhancement technique recently proposed in CNN [30], we design a squeeze-and-excitation module to fuse multi-channel node embeddings.

Specifically, we use $\mathbf{H}^k \in \mathbb{R}^{L \times N \times M}$ to denote the tensor of concatenated node embeddings of the k -th layer, where L is the number of channel, N is the number of node and M is the embedding size. The squeeze-and-excitation module consists of a squeeze and a excitation operation. First, the squeeze operation $\gamma^k = F_{sq}(\mathbf{H}^k)$ reduces \mathbf{H}^k to a channel-wise feature vector $\gamma^k \in \mathbb{R}^L$. Then, the excitation operation computes the importance weights of each channel $\alpha^k = F_{ex}(\gamma^k)$, $\alpha^k \in \mathbb{R}^L$. The squeeze operation allows this module to access global feature, while the excitation operation models the interaction of different channels and improves the expressiveness of this module.

Empirically, we find global average pooling works well as squeeze operation, and 2-layer MLP with ReLU activation works well as excitation operation. Therefore, the channel-wise importance weights

can be computed as:

$$\gamma^k = \text{GLOBAL_AVERAGE}(\mathbf{H}^k), \quad \alpha^k = \text{ReLU}(\mathbf{W}_2^k \cdot \text{ReLU}(\mathbf{W}_1^k \cdot \gamma^k)),$$

where \mathbf{W}_1^k and \mathbf{W}_2^k are two learnable matrices with $\mathbb{R}^{L \times L}$ size. The node embeddings of different channels are fused together by a sum operation weighted with α^k .

5 Theoretical Analysis

Here, we theoretically analyze the expressiveness of designed AE filter, i.e., whether it can learn distinct embeddings for nodes with different AE multisets. Specifically, we aim to answer two questions: 1) under what conditions will the AE filter be expressive enough? 2) how should that inform our design choice? Specifically, our answer to the first question is the following theorem.

Theorem 5.1 *For countable feature space \mathcal{X} , let v_a and v_b be two nodes with different AE multisets. If $\text{AGG}(\cdot)$ is an injective function on multiset, there exist some injective functions $\psi(\cdot)$ that allow automorphic equivalence filter to discriminate the two nodes with distinct node embedding.*

The proof is given in the Appendix C. In order to make AE filter expressive enough, we need to design an injective function on multiset $\text{AGG}(\cdot)$ and use a learnable function to approximate $\psi(\cdot)$. The recently developed “deep set” theory provides a framework for injective functions on set data [31], which is then extended to multiset scenario showing sum operator is an injective function on multiset [7]. Besides, the universal approximation theorem suggest that we can use multi-layer perception (MLP) with at least one hidden layer to approximate the function $\psi(\cdot)$ [32]. Therefore, based on theorem 5.1, we provide one simple design of expressive AE filter as follow.

$$h_l^k(v_t) = \text{MLP} \left(\sum_j \beta_{l,j} \cdot \text{SUM}(\{h_l^{k-1}(v_n) \mid v_n \in \mathcal{A}_{l,j}(v_t)\}) \right). \quad (3)$$

The preprocessing of identifying the AE multisets on graph data only need to run once before the network training. Therefore, its computation expense is negligible in practice. As for the model evaluation, suppose we have L subgraph templates, each template has M AE multisets and each multiset contains Q nodes on average, the overall time complexity is $\mathcal{O}(|\mathcal{V}|LMQ)$, where $|\mathcal{V}|$ is the number of nodes on graph. Empirically, the matched neighbor of each subgraph is a subset of each node’s neighborhood, i.e., $MQ \leq |\mathcal{N}|$. Therefore, the overall time complexity of GRAPE is comparable to the popular MPNNs, e.g. GraphSAGE and GCN.

6 Experiments

We conduct experiments to empirically validate GRAPE’s representational power on real-world datasets. Besides, we also analyze the behavior of the designed modules to gain more insights.

Datasets. We evaluate the models on three types of real-world datasets, i.e., academic citation networks, social networks and e-commerce co-purchase network.

- *Citation networks* [33]: We consider 2 widely used citation networks, i.e. Cora and Citeseer. In these datasets, nodes represent academic papers and (undirected) edges denote the citation links between them. Following the setting in previous work [1], we use each paper’s bag-of-words vector as its node feature and the subject as its label.
- *Social networks* [34]: We use 5 real-world social networks which are collected from the Facebook friendships within 5 universities, i.e., Hamilton, Lehigh, Rochester, Johns Hopkins (JHU) and Amherst. The nodes represent students and faculties in these universities. Besides, we use one-hot encoding of their gender and major as node feature, and set the labels as their enrollment years.
- *E-commerce co-purchase networks* [35]: This dataset was collected by crawling the *music* items in Amazon website. If an item x is frequently co-purchased with y , the graph contains a directed edge from x to y . We use the average ratings of items as node labels, and we set the node features as the number of reviews and downloads.

The detailed statistics of these datasets are presented in Appendix D.

Baselines. We compare our models with several state-of-the-art GNN models, including GCN [1], GraphSAGE [3], GIN [7], GAT [13], Geniepath [16]. Specifically, GCN and GraphSAGE are two

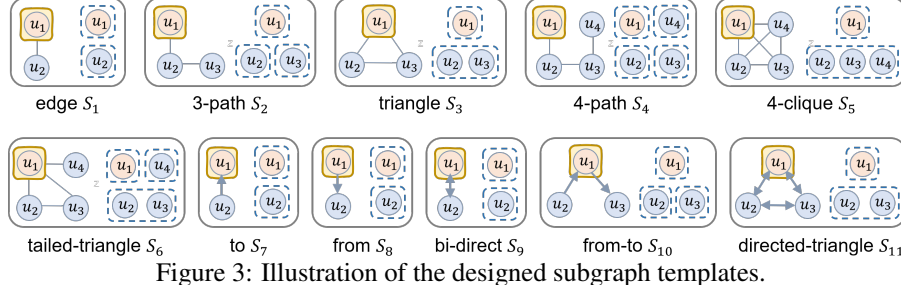


Figure 3: Illustration of the designed subgraph templates.

most popular GNN variants, and GIN is customized to better capture structural feature. Besides, GAT and Geniepath use the attention mechanism to learn adaptive neighborhood for each node. To ensure fair comparison, we follow the optimal architectures as described in previous works, and we use the official implementations released by the authors or integrated in Pytorch platform [36].

Experimental Set-up. We consider two variants of our model under the proposed framework: 1) a complete model as described in Algorithm 1 and Equation (3), which is denoted as GRAPE. 2) a simpler version of our model with the squeeze-and-excitation module replaced by an element-wise mean function, which is denoted as GRAPE-M. We use 2-layer architecture for both variants following the common design choices in previous works [1, 3, 13]. The hyper-parameter tuning and detailed experiment settings are discussed in Appendix E. Based on the prior knowledge in related areas [37, 23], we design several subgraph templates for our model, which are shown in Figure 3. Specifically, we use the subgraph templates $\{S_1, S_2, S_3, S_4, S_6\}$ for citation networks, $\{S_1, S_2, S_3, S_5, S_6\}$ for social networks and $\{S_7, S_8, S_9, S_{10}, S_{11}\}$ for e-commerce network. We discuss the motivations for these templates in Appendix F.

6.1 Main Results

We summarize the proposed models and all state-of-the-art baselines' classification accuracy on test sets in Table 1. We observe that the variants of GRAPE outperform all baseline models on each dataset. Specifically, the best-performing variants of GRAPE lead to 13.8%~60.9% relative accuracy gain over the best baseline models on social datasets. On the other hand, the margins of accuracy improvement are smaller yet still significant on citation and E-commerce datasets. One plausible explanation is the complex structural features play more important roles in social network analysis, which echos previous studies in this area [23]. We show the computation complex of each GNN variants in terms of wall-clock training time in Figure 4. Note that both Geniepath and GAT leverage attention mechanism, which can only be trained on CPU since they cause out-of-memory error in GPU training. Therefore, they take much more time to train and are not comparable to other models. In Figure 4 (a) and (d), we observe GRAPE variants take comparable time to train as other classic GNNs on two example datasets, which demonstrates the efficiency of our model.

Table 1: Classification accuracy on test sets (%). The best-performing GNNs are in boldface.

Model	Social					Citation		Ecomm.
	Hamilton	Lehigh	Rochester	JHU	Amherst	Cora	Citeseer	Amazon
GCN	19.4 \pm 2.0	24.0 \pm 1.2	21.1 \pm 1.5	20.5 \pm 0.8	17.0 \pm 1.4	86.9 \pm 1.7	74.8 \pm 1.0	47.4 \pm 1.3
GraphSAGE	20.5 \pm 2.0	17.8 \pm 2.2	18.5 \pm 1.8	17.1 \pm 2.5	17.8 \pm 1.6	85.6 \pm 0.9	70.3 \pm 1.3	19.6 \pm 1.0
GAT	18.3 \pm 2.1	22.7 \pm 0.9	20.2 \pm 1.6	19.8 \pm 1.4	17.7 \pm 2.2	82.1 \pm 2.1	74.2 \pm 1.7	38.7 \pm 0.8
GIN	23.7 \pm 5.1	19.0 \pm 2.0	21.2 \pm 0.9	21.5 \pm 3.5	26.3 \pm 6.8	86.5 \pm 1.2	72.6 \pm 1.5	48.5 \pm 2.5
Geniepath	19.1 \pm 1.5	22.9 \pm 1.0	21.7 \pm 1.1	19.8 \pm 1.4	17.5 \pm 1.7	81.2 \pm 1.5	69.8 \pm 1.7	57.9 \pm 0.8
GRAPE-M	31.6\pm8.5	25.1 \pm 2.9	24.5 \pm 4.2	26.7 \pm 6.8	35.2\pm3.7	87.5\pm1.2	75.2\pm1.4	58.3 \pm 1.1
GRAPE	28.1 \pm 9.1	27.3\pm3.8	25.0\pm4.8	34.6\pm4.3	32.6 \pm 8.2	87.1 \pm 1.8	74.6 \pm 1.5	58.6\pm1.4

Besides, we also analyze the learned squeeze-and-excitation weights on each channel and the filter weights. From Figure 4 (b), we observe the weight is significantly skewed to edge template S_1 in first layer, while it distributes more evenly on more complex templates in the second layer. On the other hand, Figure 4 (e) shows the weights in both layers skewed to the templates S_9 and S_{11} in Amazon dataset. We further examine the filter weights on some example templates in Figure 4 (c)

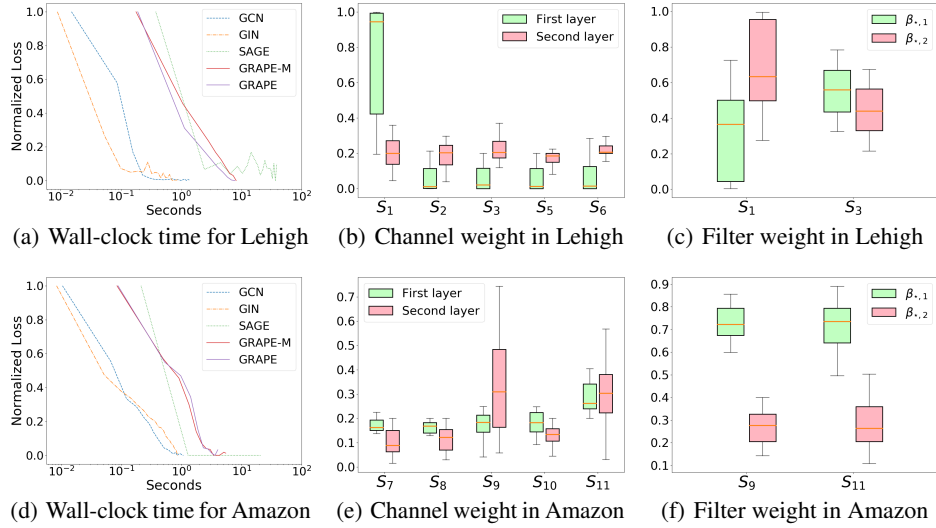


Figure 4: Illustrating the wall-clock time for training different GNN variants on two example datasets, and the channel weights and filter weights learned by GRAPE.

and (f). We observe that the AE filter can effectively distinguish the neighboring nodes with different structural roles. For example, in Lehigh dataset, GRAPE assigns lower weights to the AE multiset of ego node $\{u_1\}$ and higher weights to the AE multiset of neighbors $\{u_2\}$ on edge template S_1 , while the weights distribute more evenly between $\{u_1\}$ and $\{u_2, u_3\}$ on triangle template S_3 .

6.2 Case Study on AE Filters

We conduct a case study to better understand how the AE filters of different subgraph templates contribute to GNN framework. Specifically, we first randomly select a node v_c in *JHU* dataset that is wrongly classified by all GNN variants except GRAPE, and then analyze its 2-hop neighborhood $\mathcal{N}^2(v_c)$ and the neighboring nodes that match triangle template S_3 and 4-clique template S_5 in Figure 5 and Table 2. We observe that there are 2,782 nodes in $\mathcal{N}^2(v_c)$ and they distribute evenly on multiple labels, which not only might confuse MPNNs but also tend to cause over-smoothness problem [38]. On the other hand, both templates S_3 and S_5 significantly reduce the neighborhood size, and the percentage of neighbors that have same labels as v_c increases from 19.5% in $\mathcal{N}^2(v_c)$ (ranked 4th) to 50.0%~57.4% in $\mathcal{A}_{3,2}(v_c)$ and $\mathcal{A}_{5,2}(v_c)$ (ranked 1st). It shows the AE filter can successfully capture the “social homophily” effect, where the nodes in tightly connected communities, e.g., triangle and 4-clique structure, tend to have similar property [39].

Table 2: The number of nodes and most frequent labels in v_c ’s 2-hop neighborhood and AE multisets.

	# nodes	The percentage of top 5 labels (v_c ’s label is 17)
2-hop neigh. $\mathcal{N}^2(v_c)$	2,782	18(25.5%), 19(23.4%), 20(19.5%), 17(19.1%) , 16(6.6%)
AE multiset $\mathcal{A}_{3,2}(v_c)$	32	17(50.0%) , 18(34.4%), 16(6.3%), 19(6.3%), 20(3.1%)
AE multiset $\mathcal{A}_{5,2}(v_c)$	204	17(57.4%) , 18(29.9%), 16(7.4%), 19(4.9%), 20(0.5%)

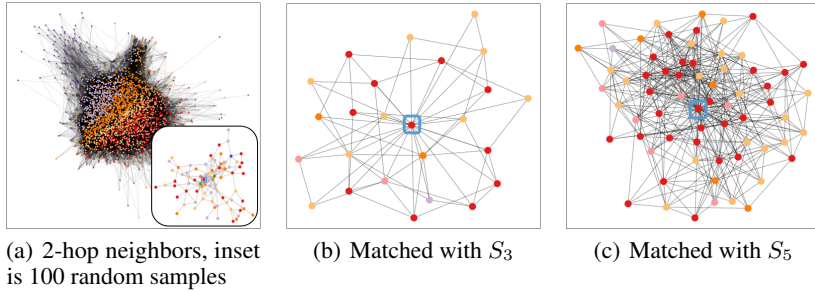


Figure 5: Case study of a node v_c in JHU dataset. The ego node v_c is positioned in the center of each subplot and circled with blue box. The node color represents the ground truth node label.

7 Conclusion

In this paper, we examine the expressiveness of MPNNs via the lens of automorphic equivalence. We theoretically prove that existing MPNNs have fundamental limitations in differentiating structural roles. To address this problem, we design a provably expressive GNN class, GRAPE, to explicitly capture the structural role with learnable automorphic equivalence filters. Experiments on eight real-world datasets suggest the proposed GRAPE has strong representational power in terms of achieving state-of-the-art performance.

Broader Impact

This work focuses on analyzing and improving graph neural network’s (GNN) representational power in distinguishing structural roles. Through the lens of automorphic equivalence, it theoretically proves that the existing local permutation invariant GNNs, such as GCN, GraphSAGE, GAT, Geniepath and GIN, have fundamental limitations in modelling the structural roles of each node’s neighbors. As a result, it proposes a novel GNN class, GRAPE, that is provably expressive in capturing the structural information encoded in automorphic equivalence. It provides a new direction for designing expressive GNN models, and might particularly benefit the downstream applications that heavily rely on structural role modelling, e.g. social network analysis and chemoinformatics.

On the other hand, applying the GRAPE framework in downstream applications may face the challenges of noisy graph data. Recent research demonstrated graph neural network are vulnerable to imperceptible noise in graph structure, which might be exploited by adversaries. Therefore, an interesting future work is to explore the adversarial attack and defense under the proposed GRAPE framework.

References

- [1] Thomas N Kipf and Max Welling. Semi-supervised classification with graph convolutional networks. In *ICLR*, 2016.
- [2] Fengli Xu, Jianxun Lian, Zhenyu Han, Yong Li, Yujian Xu, and Xing Xie. Relation-aware graph convolutional networks for agent-initiated social e-commerce recommendation. In *CIKM*, pages 529–538, 2019.
- [3] Will Hamilton, Zhitao Ying, and Jure Leskovec. Inductive representation learning on large graphs. In *NIPS*, pages 1024–1034, 2017.
- [4] Zonghan Wu, Shirui Pan, Fengwen Chen, Guodong Long, Chengqi Zhang, and S Yu Philip. A comprehensive survey on graph neural networks. *IEEE TNNLS*, 2020.
- [5] Hanjun Dai, Bo Dai, and Le Song. Discriminative embeddings of latent variable models for structured data. In *ICML*, pages 2702–2711, 2016.
- [6] Vikas K Garg, Stefanie Jegelka, and Tommi Jaakkola. Generalization and representational limits of graph neural networks. *arXiv preprint arXiv:2002.06157*, 2020.

- [7] Keyulu Xu, Weihua Hu, Jure Leskovec, and Stefanie Jegelka. How powerful are graph neural networks? *arXiv preprint arXiv:1810.00826*, 2018.
- [8] Elizabeth A Leicht, Petter Holme, and Mark EJ Newman. Vertex similarity in networks. *Physical Review E*, 73(2):026120, 2006.
- [9] Francois Lorrain and Harrison C White. Structural equivalence of individuals in social networks. *Journal of mathematical sociology*, 1(1):49–80, 1971.
- [10] Rohit Singh, Jinbo Xu, and Bonnie Berger. Global alignment of multiple protein interaction networks with application to functional orthology detection. *Proceedings of the National Academy of Sciences*, 105(35):12763–12768, 2008.
- [11] Martin G Everett. Role similarity and complexity in social networks. *Social Networks*, 7(4):353–359, 1985.
- [12] Brendan D McKay and Adolfo Piperno. Practical graph isomorphism, ii. *Journal of Symbolic Computation*, 60:94–112, 2014.
- [13] Petar Veličković, Guillem Cucurull, Arantxa Casanova, Adriana Romero, Pietro Lio, and Yoshua Bengio. Graph attention networks. Technical report, arXiv preprint arXiv:1710.10903, 2017.
- [14] Jie Hu, Li Shen, and Gang Sun. Squeeze-and-excitation networks. In *CVPR*, pages 7132–7141, 2018.
- [15] Justin Gilmer, Samuel S Schoenholz, Patrick F Riley, Oriol Vinyals, and George E Dahl. Neural message passing for quantum chemistry. In *ICML*, pages 1263–1272. JMLR. org, 2017.
- [16] Ziqi Liu, Chaochao Chen, Longfei Li, Jun Zhou, Xiaolong Li, Le Song, and Yuan Qi. Geniepath: Graph neural networks with adaptive receptive paths. In *AAAI*, volume 33, pages 4424–4431, 2019.
- [17] Jiaxuan You, Rex Ying, and Jure Leskovec. Position-aware graph neural networks. In *ICML*, pages 7134–7143, 2019.
- [18] Nima Dehmani, Albert-László Barabási, and Rose Yu. Understanding the representation power of graph neural networks in learning graph topology. In *NeurIPS*, pages 15387–15397, 2019.
- [19] Ryoma Sato, Makoto Yamada, and Hisashi Kashima. Approximation ratios of graph neural networks for combinatorial problems. In *NeurIPS*, pages 4083–4092, 2019.
- [20] Johannes Klicpera, Janek Groß, and Stephan Günnemann. Directional message passing for molecular graphs. *arXiv preprint arXiv:2003.03123*, 2020.
- [21] Narciso Pizarro. Structural identity and equivalence of individuals in social networks: beyond duality. *International Sociology*, 22(6):767–792, 2007.
- [22] Nir Atias and Roded Sharan. Comparative analysis of protein networks: hard problems, practical solutions. *Communications of the ACM*, 55(5):88–97, 2012.
- [23] Robert A Hanneman and Mark Riddle. Introduction to social network methods, 2005.
- [24] Boris Weisfeiler and Andrei A Lehman. A reduction of a graph to a canonical form and an algebra arising during this reduction. *Nauchno-Technicheskaya Informatsia*, 2(9):12–16, 1968.
- [25] Ron Milo, Shai Shen-Orr, Shalev Itzkovitz, Nadav Kashtan, Dmitri Chklovskii, and Uri Alon. Network motifs: simple building blocks of complex networks. *Science*, 298(5594):824–827, 2002.
- [26] Hong Huang, Jie Tang, Sen Wu, Lu Liu, and Xiaoming Fu. Mining triadic closure patterns in social networks. In *WWW*, pages 499–504, 2014.
- [27] Martin G Everett, John P Boyd, and Stephen P Borgatti. Ego-centered and local roles: A graph theoretic approach. *Journal of Mathematical Sociology*, 15(3-4):163–172, 1990.
- [28] Olaf Sporns and Rolf Kötter. Motifs in brain networks. *PLoS biology*, 2(11), 2004.
- [29] Alex Krizhevsky, Ilya Sutskever, and Geoffrey E Hinton. Imagenet classification with deep convolutional neural networks. In *NIPS*, pages 1097–1105, 2012.
- [30] Jie Hu, Li Shen, Samuel Albanie, Gang Sun, and Enhua Wu. Squeeze-and-excitation networks. *IEEE TPAMI*, 2017.
- [31] Manzil Zaheer, Satwik Kottur, Siamak Ravanbakhsh, Barnabas Poczos, Russ R Salakhutdinov, and Alexander J Smola. Deep sets. In *NIPS*, pages 3391–3401, 2017.

- [32] Kurt Hornik, Maxwell Stinchcombe, Halbert White, et al. Multilayer feedforward networks are universal approximators. *NN*, 2(5):359–366, 1989.
- [33] Prithviraj Sen, Galileo Namata, Mustafa Bilgic, Lise Getoor, Brian Galligher, and Tina Eliassi-Rad. Collective classification in network data. *AI Magazine*, 29(3):93–93, 2008.
- [34] Amanda L Traud, Peter J Mucha, and Mason A Porter. Social structure of facebook networks. *Physica A: Statistical Mechanics and its Applications*, 391(16):4165–4180, 2012.
- [35] Jure Leskovec, Lada A Adamic, and Bernardo A Huberman. The dynamics of viral marketing. *ACM Transactions on the Web (TWEB)*, 1(1):5–es, 2007.
- [36] Adam Paszke, Sam Gross, Francisco Massa, Adam Lerer, James Bradbury, Gregory Chanan, Trevor Killeen, Zeming Lin, Natalia Gimelshein, Luca Antiga, et al. Pytorch: An imperative style, high-performance deep learning library. In *NeurIPS*, pages 8024–8035, 2019.
- [37] Austin R Benson, David F Gleich, and Jure Leskovec. Higher-order organization of complex networks. *Science*, 353(6295):163–166, 2016.
- [38] Qimai Li, Zhichao Han, and Xiao-Ming Wu. Deeper insights into graph convolutional networks for semi-supervised learning. In *AAAI*, 2018.
- [39] Miller McPherson, Lynn Smith-Lovin, and James M Cook. Birds of a feather: Homophily in social networks. *Annual review of sociology*, 27(1):415–444, 2001.
- [40] Diederik P Kingma and Jimmy Ba. Adam: A method for stochastic optimization. In *ICLR*, 2014.

A Expressiveness of Other MPNN Variants

There have been several attempts to improve MPNN framework's expressiveness in capturing graph structural information [17, 18, 20, 19]. Here, we discuss their expressiveness in modelling the AE multisets.

Graph stethoscope [18]: This model aims to improve MPNN's power to capture graph moment, which is an important characteristic to infer the graph generation model. The researchers found MPNNs with homogeneous aggregate functions are restrictive in learning this property. Therefore, they propose a modular approach, *graph stethoscope*, to integrate heterogeneous aggregate functions. However, the proposed model preserves the local permutation invariance property of MPNN [18], which means it exhibits the same limitations as described in Proposition 3.2. Therefore, the *graph stethoscope* cannot adequately model the AE multisets.

DimeNet [20]: This model is designed to consider the spatial direction from one atom to another in molecular graphs, which is an important structural property to predict the molecule's characteristics. *DimeNet* proposes to encode the spatial direction of each edge into the passed messages, which can only be applied to the graphs where the angles between edges are known. Therefore, it cannot effectively capture the structural information in general graph data, where the angle information is often unknown.

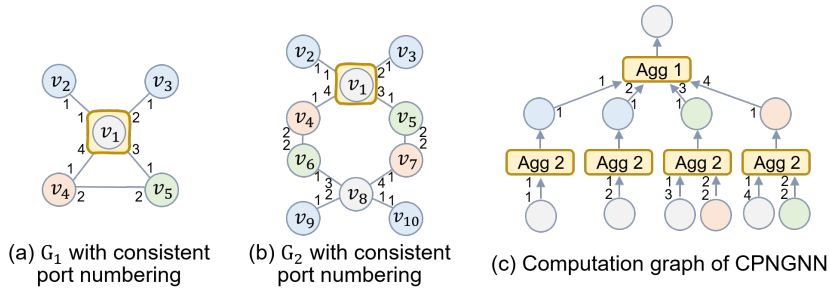


Figure 6: The limitations of CPNGNN in modelling AE multisets. Each node's feature is denoted by its color.

CPNGNN [19]: Inspired by the distributed local algorithm, the *CPNGNN* proposes to number the neighbors with *consistent port numbering*. Specifically, *port numbering* is a function p that associates each edge (v_i, v_j) with a pair of numbers (a, b) , $a \in [\text{degree}(v_i)], b \in [\text{degree}(v_j)]$, where $p(v_i, a) = (v_j, b)$ means node v_i is connected to v_j via port a . We say p is *consistent* if $p(p(v_i, a)) = (v_i, a)$ for all (v_i, a) . There might be multiple *consistent port numbering* for a given graph, CPNGNN arbitrarily chooses one for representation learning. Therefore, the *consistent port numbering* allows *CPNGNN* to treat the neighbors differently, which improves its capacity in solving combination optimization problem on graph [19]. However, we have the following proposition about its limitation in modelling AE multisets.

Proposition A.1 *There exist graphs that have different AE multisets for the ego node, but CPNGNN cannot distinguish them with some feasible consistent port numbering.*

We give a constructive proof in Figure 6. We know from Figure 1 that graph G_1 and G_2 have different AE multisets for their ego nodes. However, Figure 6(a-b) show a *consistent port numbering* for each graph that result in identical 2-layer computation graph in Figure 6(c). In fact, each node in G_2 can be mapped to a node in G_1 that has identical feature distribution and port numbering in its 1-hop neighborhood, e.g., V_8 in G_2 can be mapped to v_1 in G_1 so that they both connect to two blue neighbors via port 1~2, one green neighbor via port 3, and one red neighbor via port 4. Therefore, CPNGNN with arbitrary layer will have identical computation graphs the ego nodes in G_1 and G_2 . As a result, CPNGNN also has fundamental limitations in modelling AE multisets.

P-GNN [17]: This model aims to better encode the graph position information in the node representations. Specifically, it first randomly selects a subset of nodes as *anchors*, and then measure each node's distance to these anchors as a reference of its position on graph and encode them in its representation. Therefore, *P-GNN* is optimized to distinguish nodes with different positions on

graph instead of structural roles, which limits its capacity in modelling AE multisets. We present its performance on the experiment datasets in Table 3. We use the official implementations released by the authors [17], and follow the same experiment setting and hyper-parameter tuning as the other baselines. We observe that the *P-GNN* has significant lower classification accuracy compared with our *GRAPE* across all datasets.

Table 3: The classification accuracy of P-GNN(%).

Model	Social					Citation		Ecomm.
	Hamilton	Lehigh	Rochester	JHU	Amherst	Cora	Citeseer	Amazon
P-GNN	2.6±1.0	2.9±0.5	2.0±0.7	2.0±0.5	2.6±1.0	17.1±1.4	16.2±1.3	3.9±0.5

B Identifying AE Multisets

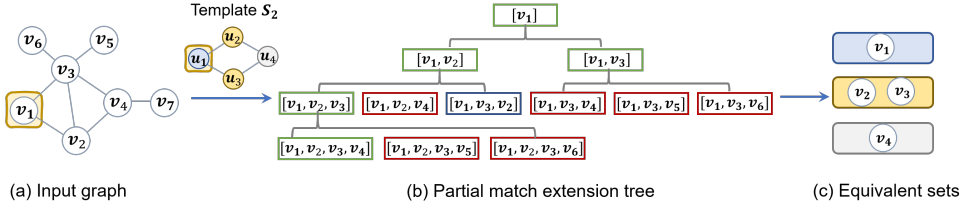


Figure 7: Illustration of identifying AE multisets.

To accelerate the matching from the subgraph template to each node’s neighborhood, we propose to maintain a partial match and recursively extend the partial match to include a neighbor of currently matched nodes. After each extension, we check the connectivity between the newly included neighbors and the already matched nodes, and leave out the partial matches that are not consistent with the template. This matching method allows us to avoid the subsets of nodes that not connected and abort the partial matches with wrong connectivity patterns in early stages, which effectively accelerates the matching process.

As exemplified in Figure 7, we first match u_1 to v_1 to initiate the partial match, then we recursively include new neighbors to form a partial match extension tree in panel (b). The red box means the connectivity patterns among the matched nodes are different from the template, e.g., $[v_1, v_2, v_4]$ and $[u_1, u_2, u_3]$. Besides, to avoid the duplicates of automorphisms such as $[v_1, v_2, v_3, v_4]$ and $[v_1, v_3, v_2, v_4]$, we require the indexes of nodes that map to same AE multisets to follow an increasing order. For example, the blue box $[v_1, v_3, v_2]$ is left out because v_3 and v_2 are mapped to u_2 and u_3 that are AE in the template but their indexes do not follow an increasing order. On the other hand, the green boxes represent the legitimate partial matches and are further extended in the following layers until they are fully matched. Finally, we allocate the nodes in the matches instances into AE multisets based on their matched nodes in the template. The detailed algorithm of identifying AE multisets is described in Algorithm 2.

C Proof for Theorem 5.1

Proof. Suppose node v_a and v_b have different AE multisets $\mathcal{T}^a = \{\mathcal{A}_1^a, \dots, \mathcal{A}_j^a, \dots\}$ and $\mathcal{T}^b = \{\mathcal{A}_1^b, \dots, \mathcal{A}_j^b, \dots\}$. Without loss of generality, we assume \mathcal{A}_j^a and \mathcal{A}_j^b are two multisets of nodes that are different. Therefore, $\text{AGG}(\cdot)$ will map them to distinct embeddings y_i^a and y_j^b since it is an injective function.

Since node feature \mathcal{X} is countable, the embedding of AE multisets y is also countable. Therefore, it can be mapped to natural numbers with some function $Z : \mathcal{Y} \rightarrow \mathbb{N}$. Each node has a set of embeddings corresponding to its AE multisets $Y = \{\text{AGG}(\{\mathcal{X}(v) | v \in \mathcal{A}_j\}) | \mathcal{A}_j \in \mathcal{T}\}, Y = \{y_j\} \subset \mathcal{Y}$, where the cardinality of Y is defined by the number of AE multisets M for the given subgraph template.

Algorithm 2: Identifying AE Multisets

Input: Graph $G = (\mathcal{V}, \mathcal{E})$, node v_t , subgraph template $S_l = (\mathcal{U}, \mathcal{R})$;

Output: AE multisets $\mathcal{T}_l = \{\mathcal{A}_{l,1}, \dots, \mathcal{A}_{l,j}, \dots\}$, where $\mathcal{A}_{l,j}$ is the multiset of nodes corresponding to the j -th structural role in the subgraph template S_l ;

```

1 Function FindEquivalence( $S_l$ ):
2    $\Pi_A = \{\pi \mid \pi \in \text{nauty}(S_l), \pi(u_1) = u_1\}$  //Find all graph automorphisms with first node
      fixed.
3    $C = []$ 
4   for  $u \in \mathcal{U}$  do
5      $c = [u]$  //Initialize a new set of AE nodes.
6     for  $\pi \in \Pi_A$  do
7       if  $u \neq \pi(u)$  then
8          $c.append(\pi(u))$  //Add in one equivalence node.
9          $\mathcal{U}.remove(\pi(u))$ 
10      end
11       $C.append(c)$  //Add the set of AE nodes to result.
12    end
13  Return  $C$ 
14 Function PartialMapExtension( $\mathcal{M}, P, \mathcal{D}, G, S_l$ ):
15   if  $\text{CheckConnectivity}(P, G, S_l)$  and  $\text{CheckNodeOrdering}(P, \mathcal{D})$  then
16     if  $|P| == |\mathcal{U}|$  then
17        $\mathcal{M}.insert(P)$ 
18     else
19        $\mathcal{D}.extend(\{v_l \mid v_l \in \mathcal{V}, v_n \in \mathcal{D}, (v_l, v_n) \in \mathcal{E}\})$  //include new neighbors.
20       for  $v_l \in \mathcal{D}$  do
21          $P.append(v_l), \mathcal{D}.remove(v_l)$ 
22          $\text{PartialMapExtension}(\mathcal{M}, P, \mathcal{D}, G, S_l)$ 
23          $P.pop\_back(), \mathcal{D}.insert(v_l)$ 
24       end
25     end
26 Function MapSubgraphTemplate( $S_l, G, v_t$ ):
27    $C = \text{FindEquivalence}(S_l)$ 
28    $\mathcal{T}_l = \{\emptyset \mid c \in C\}$ //Initialize an empty AE multiset for each set of AE nodes in template.
29    $\mathcal{D} = \{v_l \mid v_l \in \mathcal{V}, (v_l, v_t) \in \mathcal{E}\}$  //Find all neighbors as candidate of extension.
30    $P = [v_t]$ 
31    $\mathcal{M} = \emptyset$ 
32   for  $v_l \in \mathcal{D}$  do
33      $P.append(v_l), \mathcal{D}.remove(v_l)$ 
34      $\text{PartialMapExtension}(\mathcal{M}, P, \mathcal{D}, G, S_l)$ 
35      $P.pop\_back(), \mathcal{C}.insert(v_l)$ 
36   end
37   for  $P \in \mathcal{M}$  do
38      $\text{AllocateNodes}(P, \mathcal{D}, \mathcal{T}_l)$  //Allocate nodes based on the matched nodes in templates.
39   end
40  Return  $\mathcal{T}_l$ 

```

We can construct a function $f(y) = M^{-Z(y)}$ so that $\sum_{j \in [1, M]} \beta_j f(y_j), y_j \in Y$ is unique for each set of embeddings, i.e., $\sum_{j \in [1, M]} \beta_j f(\cdot)$ is an injective function on Y [31].

Therefore, for any injective function $g(\cdot)$, the $g(\sum_{j \in [1, M]} \beta_j f(\text{AGG}(\{\mathcal{X}(v) \mid v \in \mathcal{A}_j\})))$ can learn distinct embedding for v_a and v_b , since the composition of three injective functions is still an injective function. If we use $\psi(\cdot)$ to denote $g \circ f$, then it is equivalence to $\psi(\sum_{j \in [1, M]} \beta_j \text{AGG}(\{\mathcal{X}(v) \mid v \in \mathcal{A}_j\}))$, where $\psi(\cdot)$ is an injective function since both $f(\cdot)$ and $g(\cdot)$ are injective. Therefore, there exist some injective functions $\psi(\cdot)$ that allow the AE filter to learn distinct node embedding for v_a and v_b . Note that since the initial node feature \mathcal{X} is countable and the AE filter is injective, the hidden

embeddings $h^{k-1}(v)$, $k \in [2, K]$ is also countable. Therefore, this argument holds for AE filters in all hidden layers as described in Equation (2).

D Dataset Statistics

Table 4: The summary of basic statistics in the experiment datasets.

Dataset	Scenarios	Type	#Nodes	#Edges	#Triangles	#Label classes
Hamilton	Social graph	Undirected	2,116	174,972	802,803	15
Lehigh	Social graph	Undirected	4,627	358,614	1,423,036	17
Rochester	Social graph	Undirected	4,140	290,610	1,116,819	19
JHU	Social graph	Undirected	4,534	329,574	1,394,053	23
Amherst	Social graph	Undirected	2,021	162,984	799,540	15
Cora	Citation graph	Undirected	2,708	10,556	1,630	7
Citeseer	Citation graph	Undirected	3,327	9,228	1,167	7
Amazon	E-commerce graph	Directed	7,732	19,680	3,999	6

We leverage real-world datasets collected from three scenarios, i.e., social graph¹, citation graph², and e-commerce graph³. All these datasets can be publicly accessed through the links in footnote, and the basic statistics are summarized in Table 4. The datasets have wide ranges in the number of nodes, edges, triangles and label classes, which ensures the robustness of the experiment results.

E Experiment Setting and Hyper-parameter

Following the setting in previous works [7], we perform a grid search on the following hyper-parameters: 1) embedding size $\in \{16, 32\}$; 2) the dropout rate $\in \{0.3, 0.5\}$; 3) L2 regularization coefficient $\in \{3 \cdot 10^{-5}, 5 \cdot 10^{-5}\}$; 4) initial learning rate $\in \{0.01, 0.03\}$, which is decayed by 50% for every 100 epochs. To improve the robustness of experiment results, we report the average and standard deviation of each model’s performance over 10 runs. In each run, we randomly split the datasets into 60% training set, 20% validation set and 20% test set. Specifically, we use the training set to learn the models, and report the classification performance on test set. We train each model for 500 epochs with early stopping of 50 window size, i.e. the training is terminated if the model’s performance on validation set does not improve for consecutive 50 epochs. Our model and all the baseline models are implemented in Pytorch [36] with the Adam optimizer [40]. We evaluate them on a single machine with 4 NVIDIA GeForce RTX 2080 GPUs.

F Subgraph Templates Design

We design multiple subgraph templates to allow GRAPE to capture various structural information, which are presented in Figure 3. Here, we discuss the motivations for their design.

- 1) *Edge S_1* : it captures the basic connection in graph data, and has two sets of AE nodes, i.e., $\{u_1\}$ and $\{u_2\}$. Therefore, it leads to two AE multisets: one contains the ego node itself (corresponding to u_1) and the other contains all the 1-hop neighbors (corresponding to u_2).
- 2) *3-path S_2* : it captures the 2-hop neighborhood of the ego node, and partition the neighbors into three AE multisets based on their hops from ego node, which maps to $\{u_1\}$, $\{u_2\}$ and $\{u_3\}$, respectively. In the context of citation network, it captures the documents that co-cite one document. Besides, it captures the individuals that have common friends in social network.
- 3) *Triangle S_3* : This template captures an important pattern in graph data, i.e., triangle. Based on the triadic closure theory [26, 23], this template captures the strong ties in social graph, i.e., the individuals that form triangle structure tend to have similar feeling about an object. This template maps the neighborhood into two AE multisets that corresponds to $\{u_1\}$ and $\{u_2, u_3\}$,

¹<http://arxiv.org/abs/1102.2116>

²<http://www.cs.umd.edu/~sen/lbc-proj/LBC.html>

³<http://snap.stanford.edu/data/index.html/amazon>

respectively. But differs from edge template S_1 , $\{u_2, u_3\}$ maps to the neighbors that tend to have stronger influence on ego node.

- 4) 4-path S_4 : similar to the 3-path template, this template maps the nodes in 3-hop neighborhood into 4 AE multisets based on their hops from ego node. It allows the model to access more far away features.
- 5) 4-clique S_5 : this template captures the closed connected communities in graph data, which tend to exhibit the “homophily effect” [39]. It maps the neighborhood into two AE multisets that corresponds to $\{u_1\}$ and $\{u_2, u_3, u_4\}$, respectively.
- 6) Tailed-triangle S_6 : on the basis of triangle template S_3 , this template adds an additional neighbor to the ego node. Therefore, it partitions the neighborhood into three AE multisets, i.e., $\{u_1\}$, $\{u_2, u_3\}$ and $\{u_4\}$, where $\{u_2, u_3\}$ identifies the neighbors with strong ties and $\{u_4\}$ identifies the neighbors connected by simple edge.
- 7) To S_7 : it identifies the neighbors that point to the ego node in directed graph. In the context of e-commerce co-purchase network, u_2 maps to items that often lead to the purchase of u_1 .
- 8) From S_8 : it identifies the neighbors that have directed edges from the ego node. In the context of e-commerce co-purchase network, the purchase of ego node u_1 often leads to the purchase of u_2 .
- 9) Bi-direct S_9 : it identifies the neighbors that are connected to and from the ego node, which are the intersection of the nodes identified by template S_7 and S_8 . Therefore, u_2 maps to the items that are frequently co-purchased with S_{11} .
- 10) From-to S_{10} : it maps to the unions of the nodes identified by template S_7 and S_8 . Specifically, it partitions the neighborhood into three AE multisets, i.e. $\{u_1\}$, $\{u_2\}$ and $\{u_3\}$, which correspond to the ego node itself, the nodes that point to ego node, and the nodes that are pointed from ego node, respectively.
- 11) Directed-triangle S_{11} : similar with the triangle template S_3 , this template captures the triangle patterns in directed graph setting. Specifically, it leads to two AE multisets, which correspond to $\{u_1\}$ and $\{u_2, u_3\}$, respectively.